Cite this: DOI: 00.0000/xxxxxxxxxx

Interface-induced hysteretic volume phase transition of microgels: simulation and experiment

Jannis Kolker,*[a] Johannes Harrer,‡[b] Simone Ciarella,[c] Marcel Rey,[b] Maret Ickler,[b] Liesbeth M. C. Janssen,[c] Nicolas Vogel,[b] and Hartmut Löwen[a]

Received Date
Accepted Date

DOI: 00.0000/xxxxxxxxxx

Supporting Information

1 Materials and Methods

1.1 Bead and bond potentials

The bead-bead interaction is modeled by a Weeks-Chandler-Andersen [1] potential

$$V_{\mathrm{WCA}}(r) = \begin{cases} 4\varepsilon\left[\left(\frac{\sigma}{r}\right)^{12} - \left(\frac{\sigma}{r}\right)^{6}\right] + \varepsilon & \text{if} \quad r \leq 2^{\frac{1}{6}}\sigma \\ 0 & \text{otherwise} \end{cases} \tag{1}$$

where r is the radial distance between two beads, σ represents the bead diameter and ε is the strength of repulsion. The bead-connecting covalent bonds are described by a finite-extensible-nonlinear-elastic (FENE) [2,3] potential

$$V_{\mathrm{FENE}}(r) = \begin{cases} -\tilde{k}_{\mathrm{F}}\tilde{R}_0^2 \ln\left(1 - \left(\frac{r}{\tilde{R}_0}\right)^2\right) & \text{if} \quad r < \tilde{R}_0 \\ 0 & \text{otherwise} \end{cases} \tag{2}$$

with $\tilde{k}_{\mathrm{F}} = 15\varepsilon/\sigma^2$ an effective spring constant and $\tilde{R}_0 = 1.5\sigma$ the maximal bond expansion.

1.2 Attractive interfacial energies in simulation and experiment

In the experiment, a surface tension difference $\gamma_{\mathrm{a/w}} - \gamma_{\mathrm{a/w/PNiPAm}}$ of the air/water surface tension $\gamma_{\mathrm{a/w}}$ and a surface tension of an adsorbed PNiPAm microgel $\gamma_{\mathrm{a/w/PNiPAm}}$ was measured for an interfacial layer of microgels. The surface tension difference was found to be approximately $30\frac{\mathrm{mJ}}{\mathrm{m}^2}$ at a temperature of $T^* = 293\mathrm{K}$. The interface attraction energy $\varepsilon_{\mathrm{ext}}$ for a single monomer can be calculated via

$$\varepsilon_{\mathrm{ext}} = (\gamma_{\mathrm{a/w}} - \gamma_{\mathrm{a/w/PNiPAm}})\,\pi R_{\mathrm{mono}}^2, \tag{3}$$

with $R_{\mathrm{mono}} \approx 0.5\,\mathrm{nm}$ as a typical monomer radius. Consequently, this leads to an effective interface attraction energy of $5.5\,\mathrm{k_B T^*}$, as chosen in the simulation. In principle, $\varepsilon_{\mathrm{ext}}$ should be temperature-dependent via the temperature-dependence surface tension of water but we have neglected this dependence as the surface tension only varies about less than $\pm 5\%$ within the temperature regime considered.

1.3 Comparison of a sudden and an multiple stepwise change of the effective attraction α

In order to mimick more the experimental situation of stepwise cooling and heating, we have also changed the effective attraction α in a multiple stepwise manner slower than a stepwise manner. For the crosslinking density of 2.3%, corresponding data are shown in Figure 1. While qualitative differences exist, the amount of stretching for the swollen state and the subsequent collapsed state is approximately the same. Hence, no major differences in the net hysteresis are found for different cooling and heating speeds.

[a] *Institut fur Theoretische Physik II, Heinrich-Heine-Universität Düsseldorf, Universitätsstrasse 1, D-40225 Düsseldorf, Germany.*
[b] *Institute of Particle Technology, Friedrich-Alexander University Erlangen-Nürnberg, Cauerstrasse 4, 91058 Erlangen, Germany.*
[c] *Theory of Polymers and Soft Matter, Department of Applied Physics, Eindhoven University of Technology, P.O. Box 513, 5600MB Eindhoven, The Netherlands.*

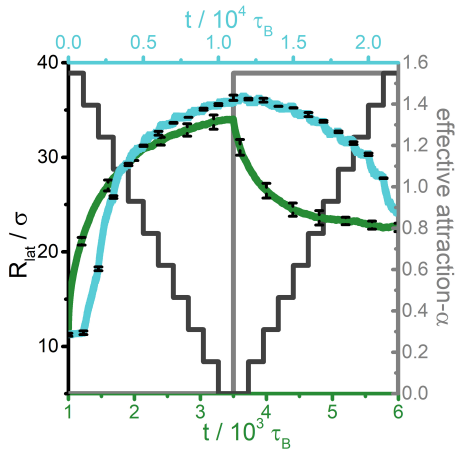

Fig. 1 Simulation data for a temperature cycling of a microgel at an interface for a multiple stepwise (black line) and a sudden (grey line) change in the effective attraction α. The sudden change (green line) and the multiple stepwise change (blue line) are reaching the same amount of stretching for the swollen state and for the subsequent collapsed state. The data are obtained for a crosslinking density of 2.3%

1.4 Core-corona structure

We characterize the internal core-corona structure of the microgel by a geometric analysis of the bead configurations. The main idea is as follows: we consider all bead positions projected to the xy-plane which have a distance less than a prescribed r from the (stationary) microgel center $\vec{R}_0$, i.e. all bead positions which fulfill $(x_i(t)-X_0(t))^2+(y_i(t)-Y_0(t))^2<r$. In the corona region we expect that the set of bead positions exhibits a relatively rough boundary while in the core region the boundary is fairly smooth.

To quantify this further we consider the convex hull around the set of bead positions which provides a contour length $L_{convex}(r)$. We also define a *concave* hull around the same bead positions and compare its contour length $L_{concave}(r)$ to $L_{convex}(r)$. Clearly, $L_{concave}(r)\geq L_{convex}(r)$. In contrast to the convex contour, the precise definition of the concave hull is not unique. In detail, for the calculation of the concave hull we employed the algorithm in Ref. [4] with the so-called k-nearest-neighbour approach where we used $k=20$.

The relative difference in the two contour lengths defines a parameter $\Delta(r)$

$$\Delta(r)=\frac{L_{\text{concave}}(r)-L_{\text{convex}}(r)}{L_{\text{concave}}(r)} \tag{4}$$

The spatial dependence of $\Delta(r)$ contains valuable information about the core size R_c and the corona size R_{co}. Inside the core Δ is small while it increases for increasing r until it saturates with a value Δ_∞ of the order of one, concomitant with a "rugged" concave hull. We can therefore extract the core and corona size approximatively by studying the behavior of $\Delta(r)$ near its inflection point at $r=r^*$ defined by the condition $d^2\Delta(r)/dr^2|_{r=r^*}=0$. Considering the tangent $\tilde{t}(r)$ through the inflection point given by the linear relation $\tilde{t}(r)=\Delta(r^*)+d\Delta(r)/dr|_{r=r^*}\times(r-r^*)$, we define the core size R_c by the intersection of the tangent with the r-axis, i.e. by the condition $\tilde{t}(R_c)=0$. The corona size is defined by the distance where the tangent reaches the saturation value Δ_∞, i.e. by the relation $\tilde{t}(R_{co})=\Delta_\infty$.

Concrete data for a typical microgel snapshot along with the profiles for $\Delta(r)$ are presented in figure 2i)-iii) corresponding to three different situations: i) initially collapsed state of a microgel particle brought to the interface from the bulk, ii) swollen microgel particle at the interface after the first temperature change, iii) collapsed state after one full cycle. The associated concave and convex hulls for the inner and outer part are indicated in different colors. Moreover, in figure 2iv)-vi) the corresponding profiles $\Delta(r)$ are presented together with the tangent $\tilde{t}(r)$ (full red line) and the determination of the core size R_c and the corona size R_{co}.

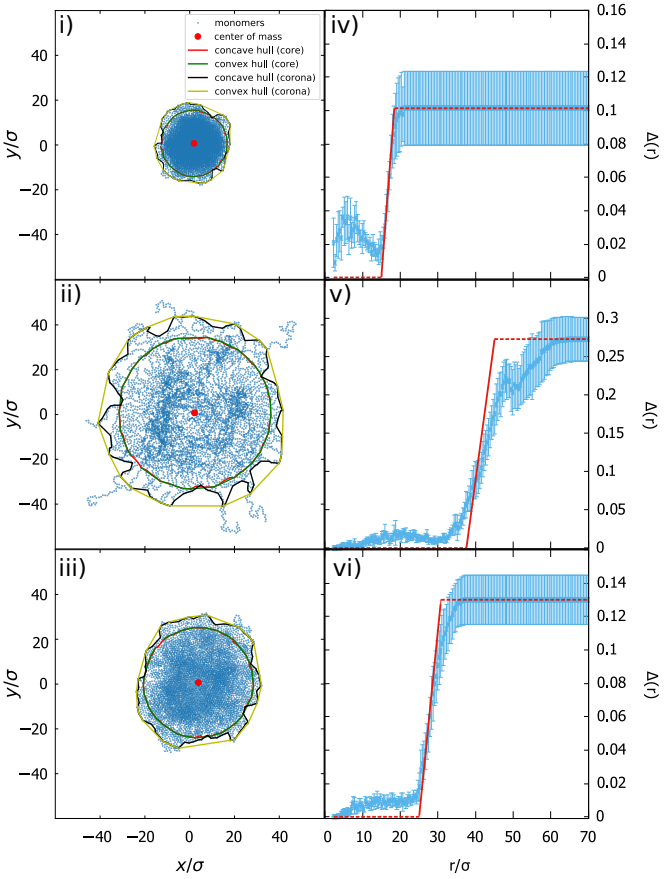

Fig. 2 i)-iii) Typical bead configurations for a crosslinking density of 4.5% at the interface (top view) for the initial collapsed state i), the swollen state ii) and the collapsed state after one cycle iii). Different hulls for the core and corona are indicated in different colors (see legend). The corresponding $\Delta(r)$-profiles are shown in iv), v) and vi) with error bars. The tangent on the $\Delta(r)$-profile is shown as a full red line, the intersection point with the dashed lines indicates the core and corona size.

Notes and references

1 J. D. Weeks, D. Chandler and H. C. Andersen, *The Journal of Chemical Physics*, 1971, **54**, 5237–5247.

2 N. Gnan, L. Rovigatti, M. Bergman and E. Zaccarelli, *Macromolecules*, 2017, **50**, 8777–8786.

3 F. Camerin, M. A. Fernandez-Rodríguez, L. Rovigatti, M.-N. Antonopoulou, N. Gnan, A. Ninarello, L. Isa and E. Zaccarelli, *ACS nano*, 2019, **13**, 4548–4559.

4 A. Moreira and M. Y. Santos, *GRAPP 2007 - 2nd International*

Conference on Computer Graphics Theory and Applications, Proceedings, 2007, **GM**, 61–68.